Electronic Supplementary Material (ESI) for Inorganic Chemistry Frontiers.

ELECTRONIC SUPPLEMENTARY INFORMATION

Pressure-induced reversible framework rearrangement and increased polarization in the polar $[NH_4][Cd(HCOO)_3]$ hybrid perovskite

Juan Manuel Bermúdez-García[a], Alberto García-Fernández[a], Adrián Andrada-Chacón[b], Javier Sánchez-Benítez[b], Wei Ren[c,d], Shunbo Hu[c,d], Gu Teng[e], Hongjun Xiang[e], Malgorzata Biczysko[f], Socorro Castro-García[a], Manuel Sánchez-Andújar[a*], Alessandro Stroppa[g*], María Antonia Señarís-Rodríguez[a]

[a] Department of Chemistry, Faculty of Sciences and CICA, University of A Coruña, Campus A Coruña, 15071 A Coruña, Spain.

[b] MALTA-Consolider Team, Departamento de Química Física, Facultad de Ciencias Químicas, Universidad Complutense de Madrid, 28040 Madrid, Spain

[c] Department of Physics and International Center of Quantum and Molecular Structures, Shanghai University, Shanghai 200444, China

[d] Materials Genome Institute, Shanghai Key Laboratory of High Temperature Superconductors, Shanghai University, Shanghai 200444, China

[e] Key Laboratory of Computational Physical Sciences (Ministry of Education), State Key Laboratory of Surface Physics, Department of Physics, Fudan University, Shanghai 200433, China

[f] International Centre for Quantum and Molecular Structures (ICQMS), College of Sciences, Shanghai University, 99 Shangda Road, 200444 Shanghai, China.

[g] CNR-SPIN, c/o Dip.to di Scienze Fisiche e Chimiche - Via Vetoio - 67010 - Coppito (AQ), Italy

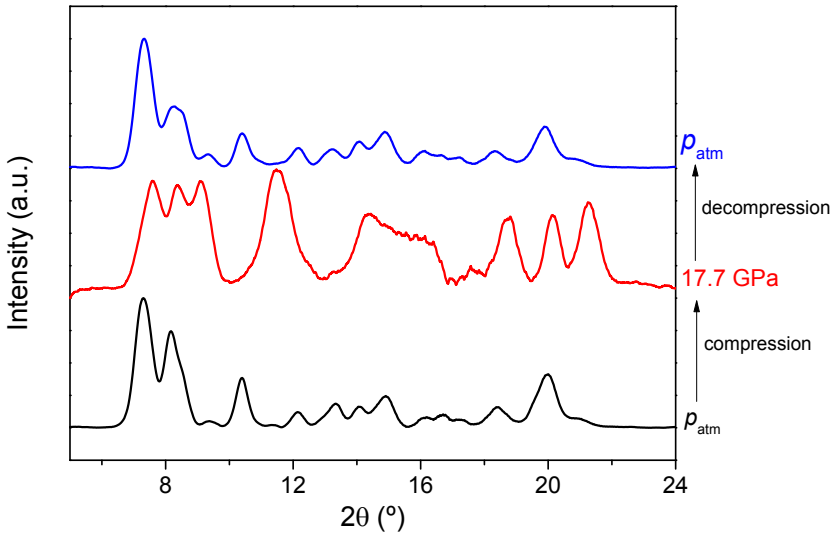

Figure S1. PXRD patterns of $[NH_4][Cd(HCOO)_3]$ upon compression (p_{atm} → 17.7 GPa) and decompression (17.7 GPa → p_{atm}) at room temperature.

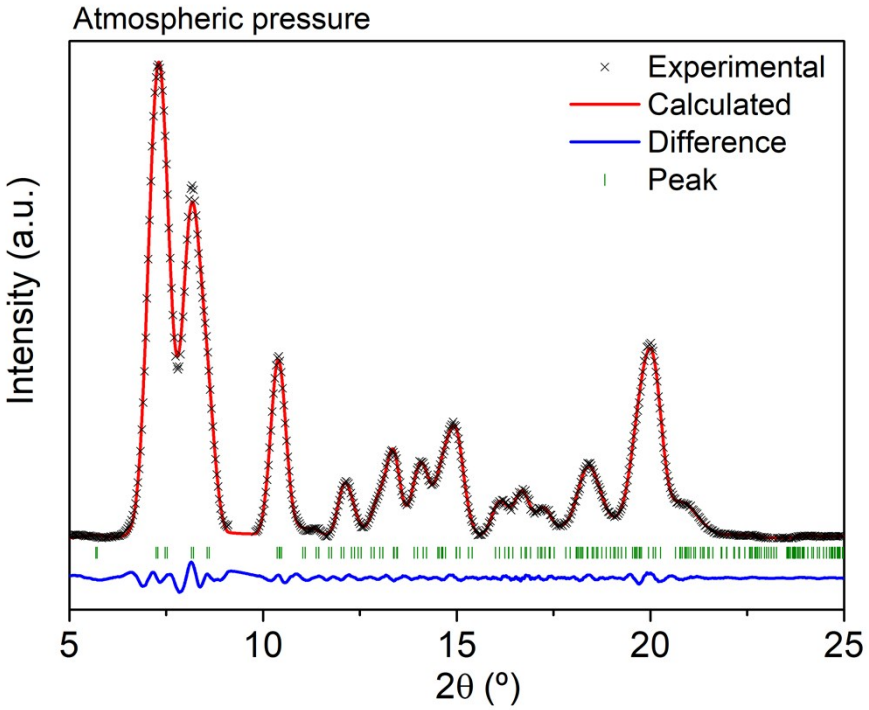

Figure S2. Le Bail fitting of X-ray powder diffraction patterns for the $[NH_4][Cd(HCOO)_3]$ at atmospheric pressure to LP-phase. Note: Experimental (black cross), calculated (red solid line) and difference (blue solid line at the bottom) profiles. The tick green marks indicate the positions of the allowed Bragg reflections.

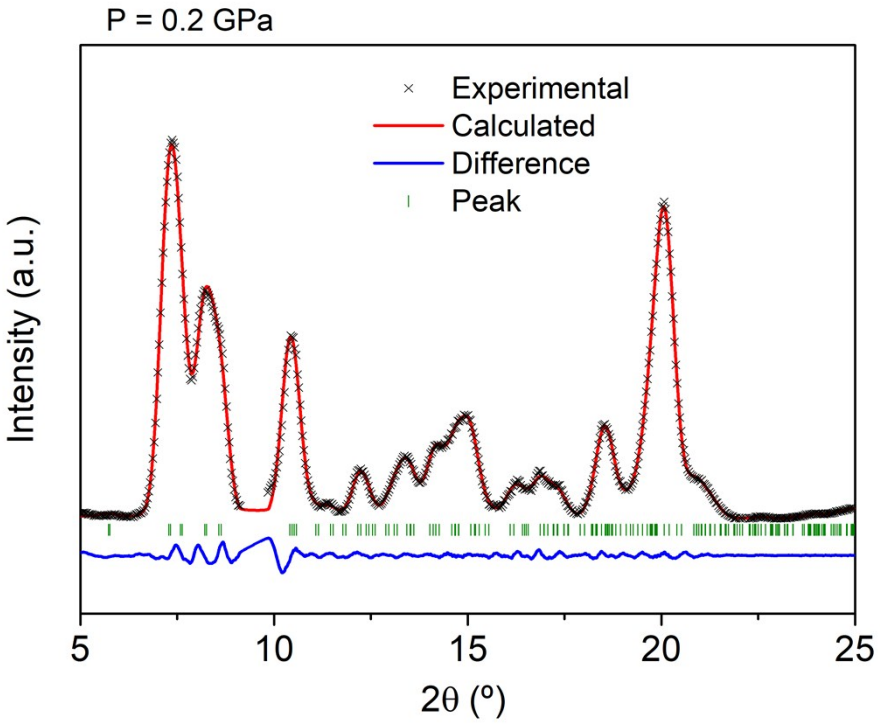

Figure S3. Le Bail fitting of X-ray powder diffraction patterns for the $[NH_4][Cd(HCOO)_3]$ at p = 0.2 GPa to LP-phase. Note: Experimental (black cross), calculated (red solid line) and difference (blue solid line at the bottom) profiles. The tick green marks indicate the positions of the allowed Bragg reflections.

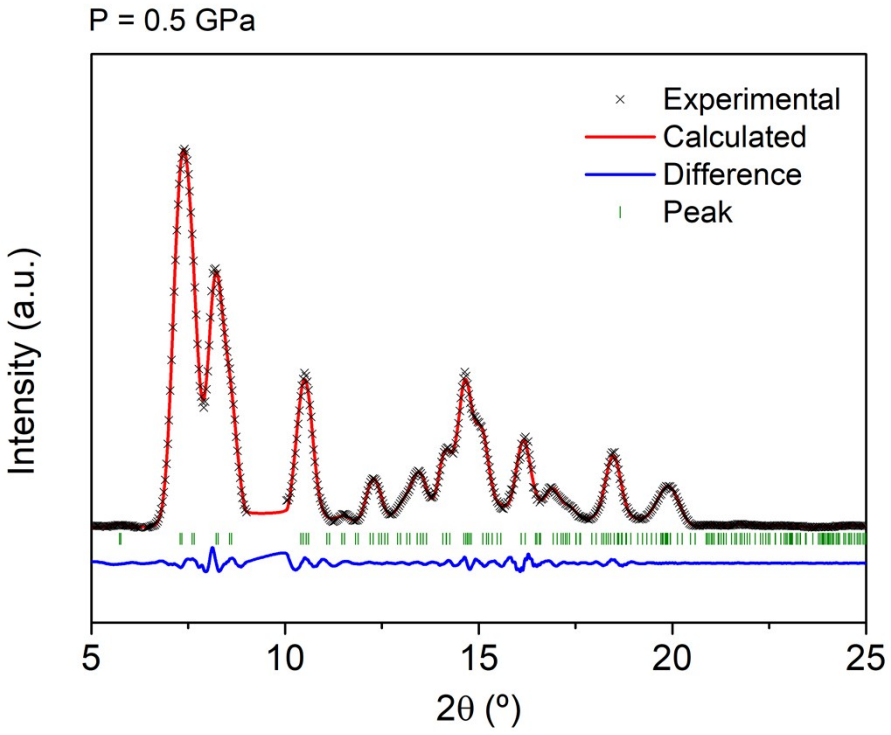

Figure S4. Le Bail fitting of X-ray powder diffraction patterns for the $[NH_4][Cd(HCOO)_3]$ at p = 0.5 GPa to LP-phase. Note: Experimental (black cross), calculated (red solid line) and difference (blue solid line at the bottom) profiles. The tick green marks indicate the positions of the allowed Bragg reflections.

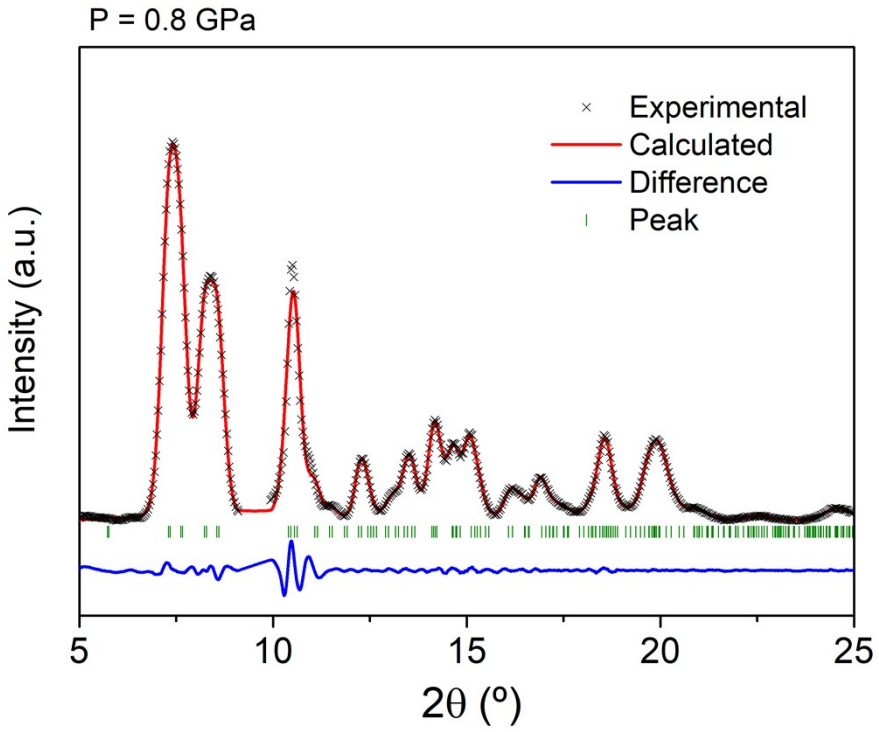

Figure S5. Le Bail fitting of X-ray powder diffraction patterns for the $[NH_4][Cd(HCOO)_3]$ at p = 0.8 GPa to LP-phase. Note: Experimental (black cross), calculated (red solid line) and difference (blue solid line at the bottom) profiles. The tick green marks indicate the positions of the allowed Bragg reflections.

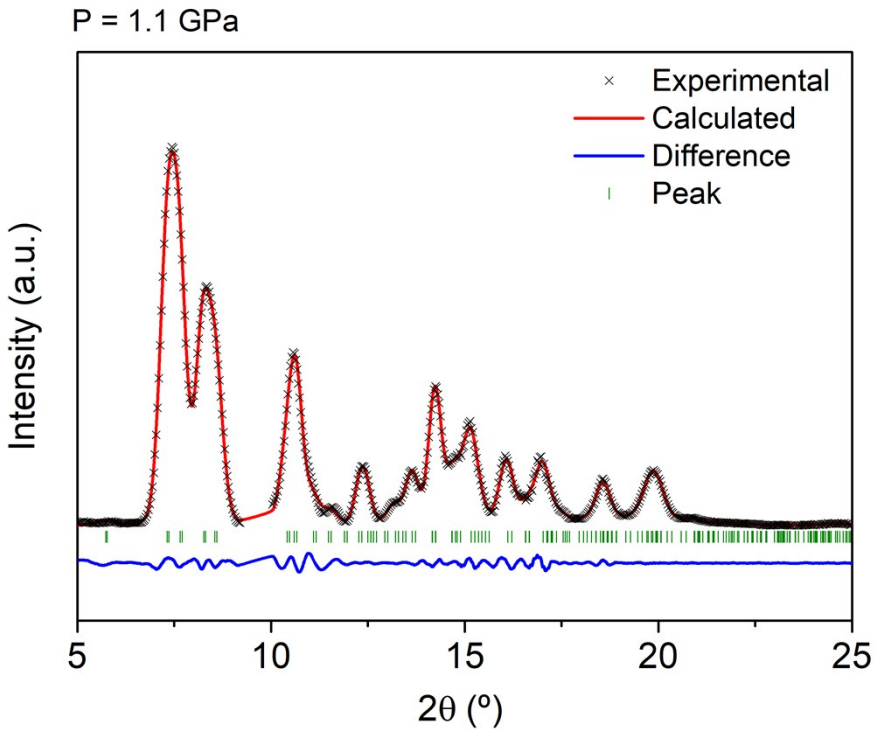

Figure S6. Le Bail fitting of X-ray powder diffraction patterns for the $[NH_4][Cd(HCOO)_3]$ at p = 1.1 GPa to LP-phase. Note: Experimental (black cross), calculated (red solid line) and difference (blue solid line at the bottom) profiles. The tick green marks indicate the positions of the allowed Bragg reflections.

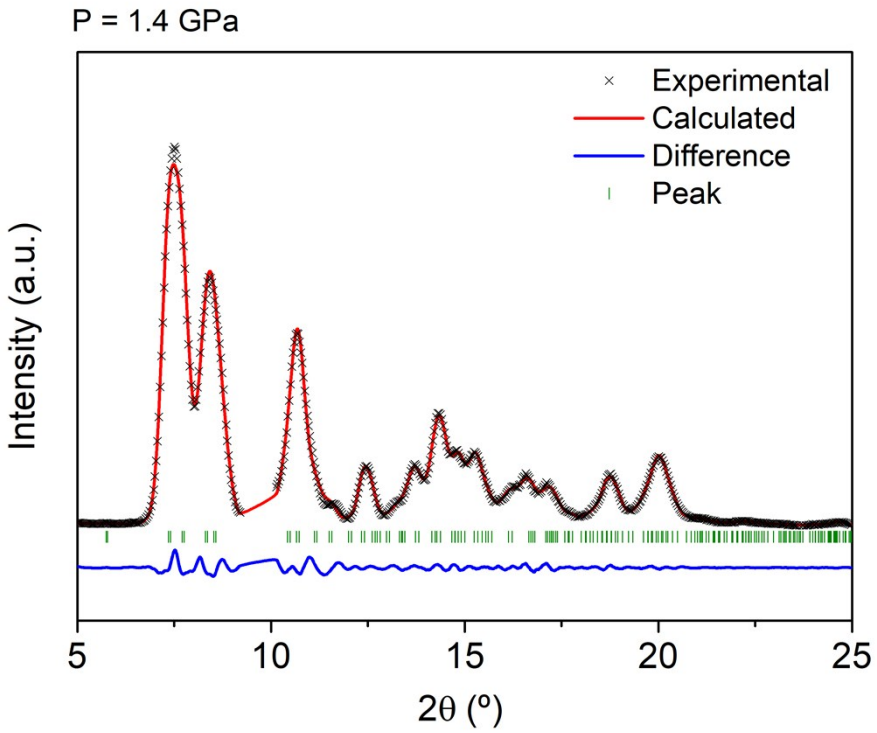

Figure S7. Le Bail fitting of X-ray powder diffraction patterns for the $[NH_4][Cd(HCOO)_3]$ at p = 1.4 GPa to LP-phase. Note: Experimental (black cross), calculated (red solid line) and difference (blue solid line at the bottom) profiles. The tick green marks indicate the positions of the allowed Bragg reflections.

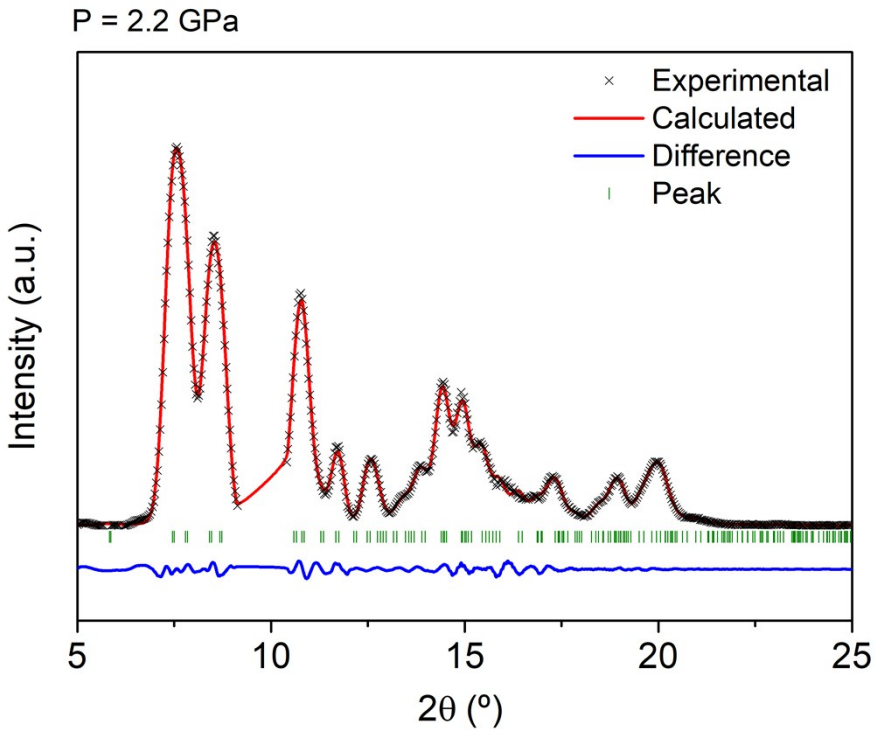

Figure S8. Le Bail fitting of X-ray powder diffraction patterns for the $[NH_4][Cd(HCOO)_3]$ at p = 2.2 GPa to LP-phase. Note: Experimental (black cross), calculated (red solid line) and difference (blue solid line at the bottom) profiles. The tick green marks indicate the positions of the allowed Bragg reflections.

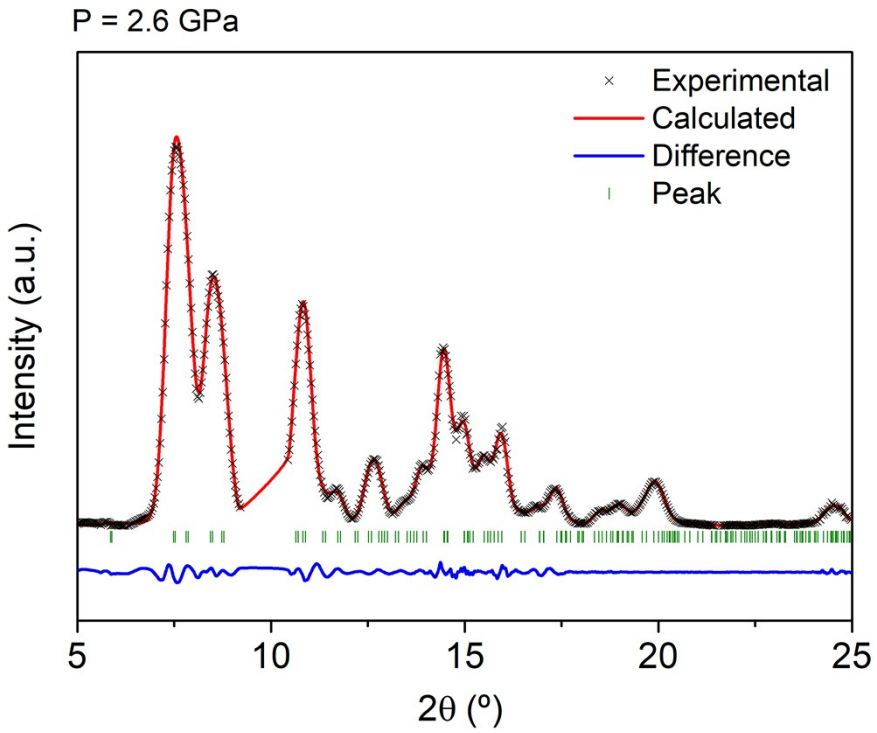

Figure S9. Le Bail fitting of X-ray powder diffraction patterns for the $[NH_4][Cd(HCOO)_3]$ at p = 2.6 GPa to LP-phase. Note: Experimental (black cross), calculated (red solid line) and difference (blue solid line at the bottom) profiles. The tick green marks indicate the positions of the allowed Bragg reflections.

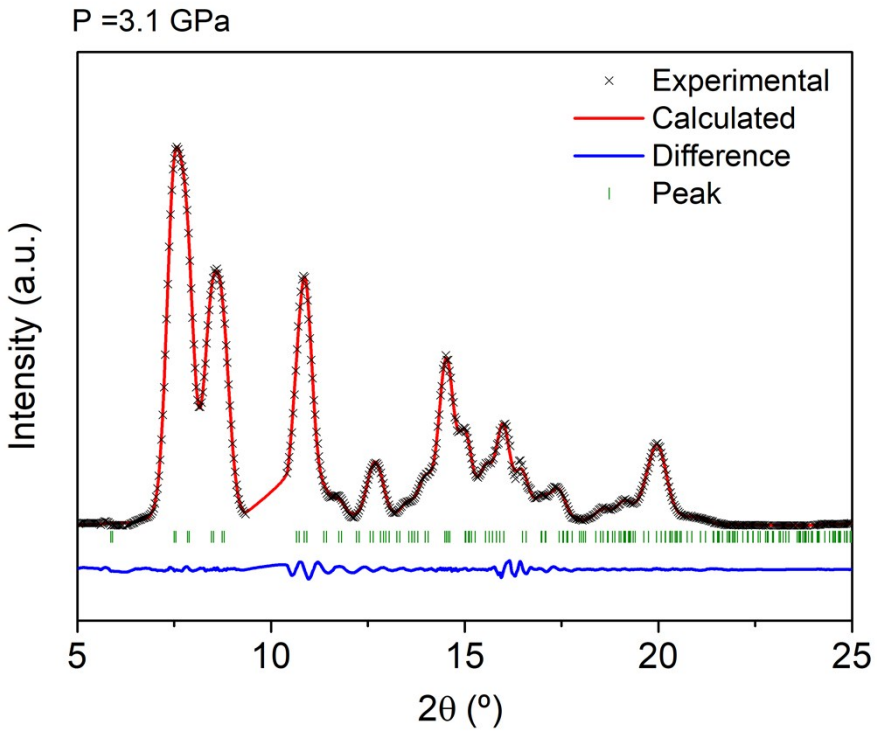

Figure S10. Le Bail fitting of X-ray powder diffraction patterns for the $[NH_4][Cd(HCOO)_3]$ at p = 3.1 GPa to LP-phase. Note: Experimental (black cross), calculated (red solid line) and difference (blue solid line at the bottom) profiles. The tick green marks indicate the positions of the allowed Bragg reflections.

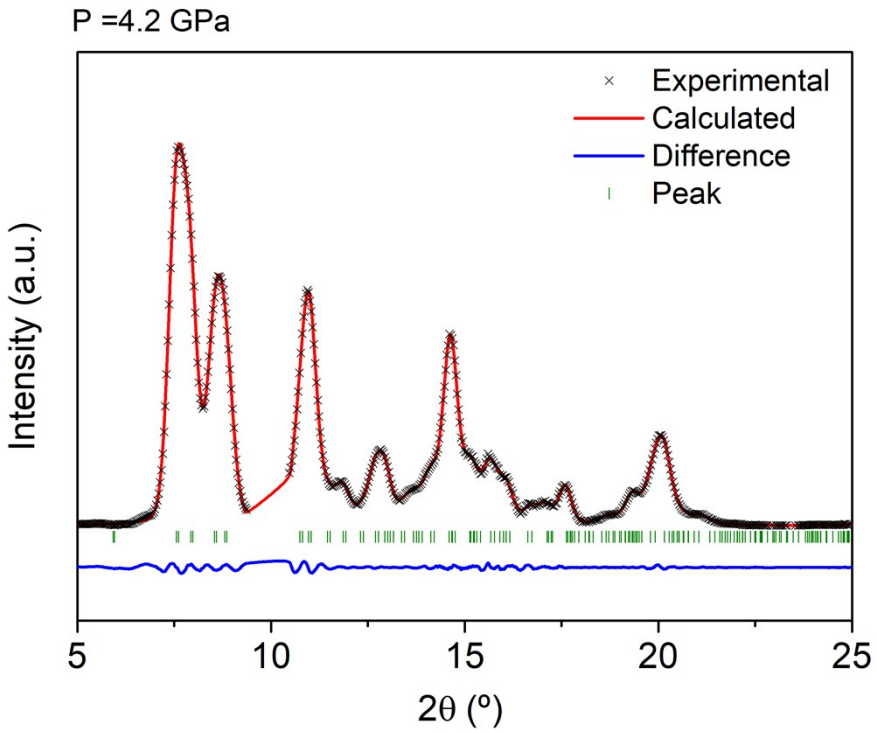

Figure S11. Le Bail fitting of X-ray powder diffraction patterns for the $[NH_4][Cd(HCOO)_3]$ at p = 4.2 GPa to LP-phase. Note: Experimental (black cross), calculated (red solid line) and difference (blue solid line at the bottom) profiles. The tick green marks indicate the positions of the allowed Bragg reflections.

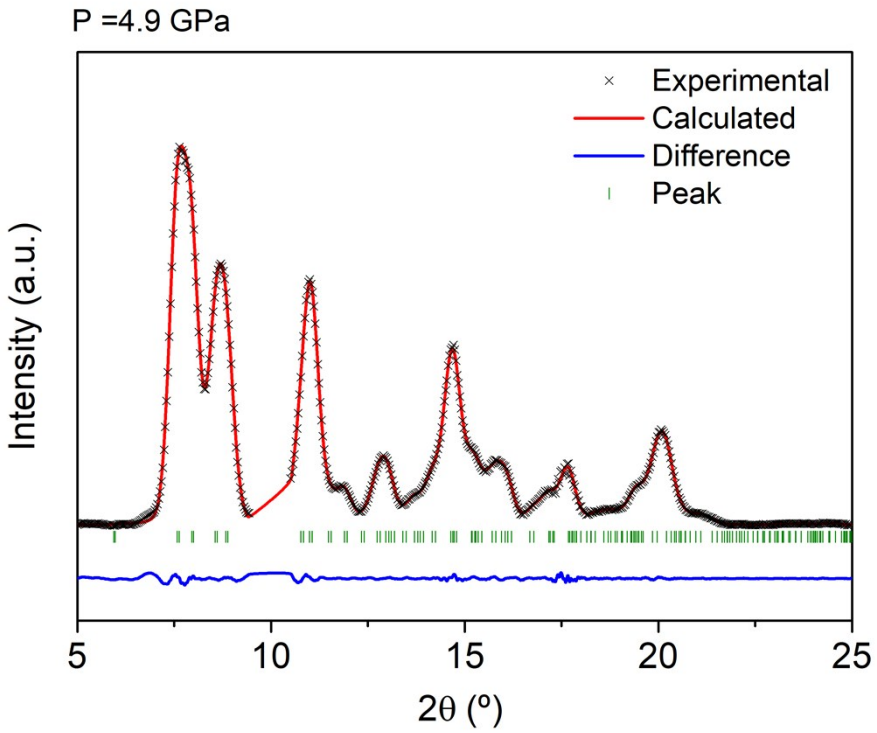

Figure S12. Le Bail fitting of X-ray powder diffraction patterns for the $[NH_4][Cd(HCOO)_3]$ at p = 4.9 GPa to LP-phase. Note: Experimental (black cross), calculated (red solid line) and difference (blue solid line at the bottom) profiles. The tick green marks indicate the positions of the allowed Bragg reflections.

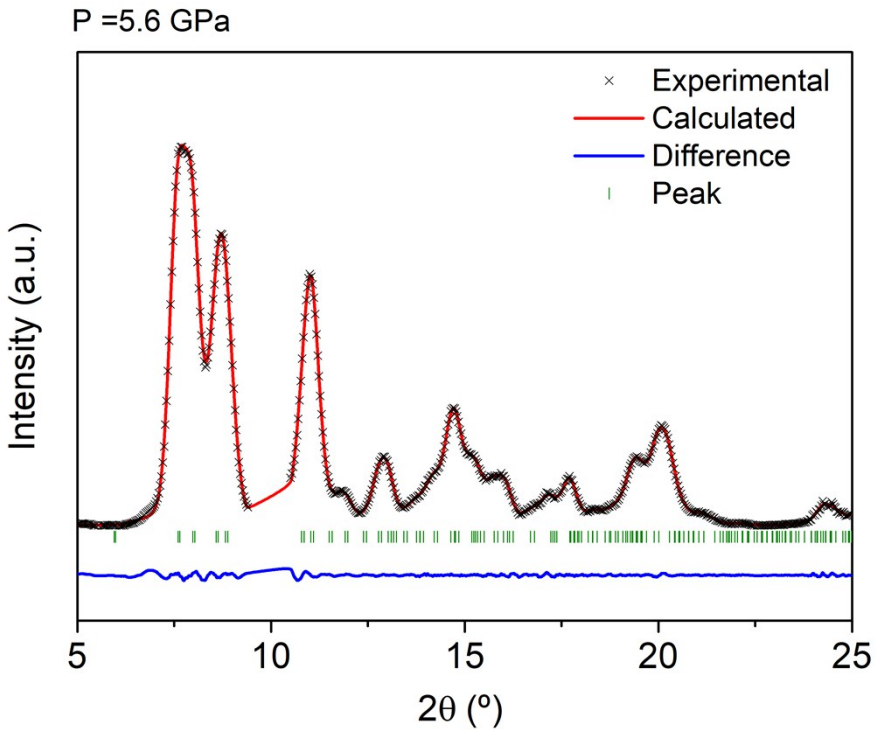

Figure S13. Le Bail fitting of X-ray powder diffraction patterns for the $[NH_4][Cd(HCOO)_3]$ at p = 5.6 GPa to LP-phase. Note: Experimental (black cross), calculated (red solid line) and difference (blue solid line at the bottom) profiles. The tick green marks indicate the positions of the allowed Bragg reflections.

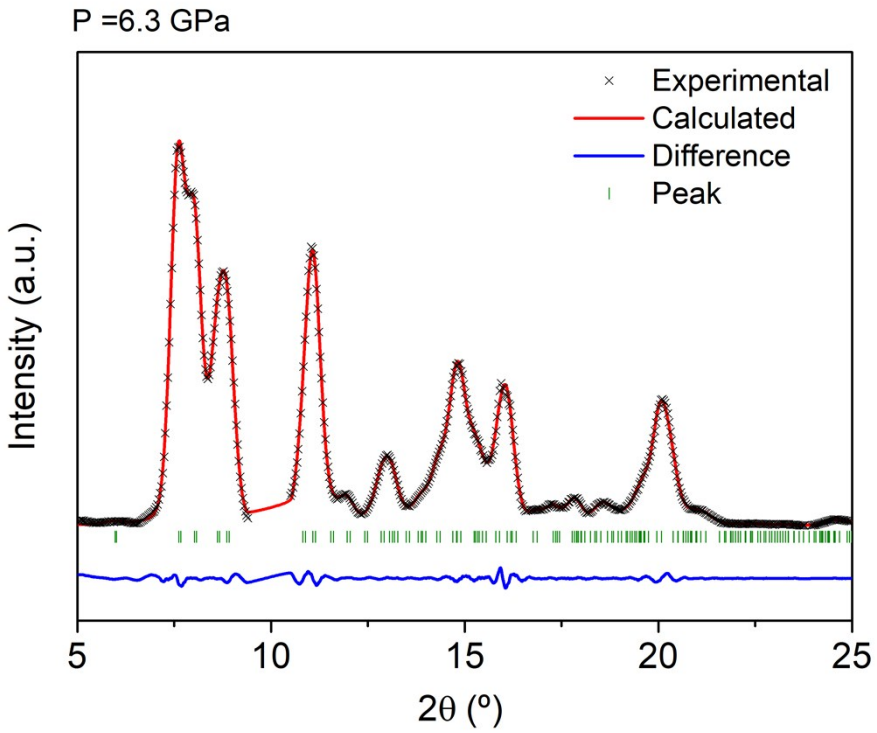

Figure S14. Le Bail fitting of X-ray powder diffraction patterns for the $[NH_4][Cd(HCOO)_3]$ at p = 6.3 GPa to LP-phase. Note: Experimental (black cross), calculated (red solid line) and difference (blue solid line at the bottom) profiles. The tick green marks indicate the positions of the allowed Bragg reflections.

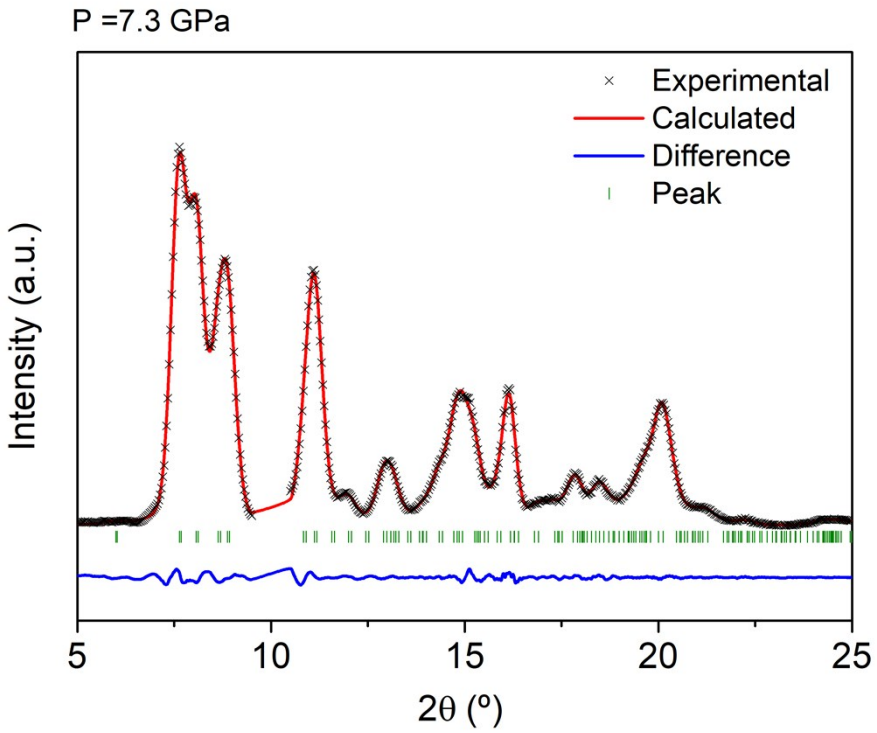

Figure S15. Le Bail fitting of X-ray powder diffraction patterns for the $[NH_4][Cd(HCOO)_3]$ at p = 7.3 GPa to LP-phase. Note: Experimental (black cross), calculated (red solid line) and difference (blue solid line at the bottom) profiles. The tick green marks indicate the positions of the allowed Bragg reflections.

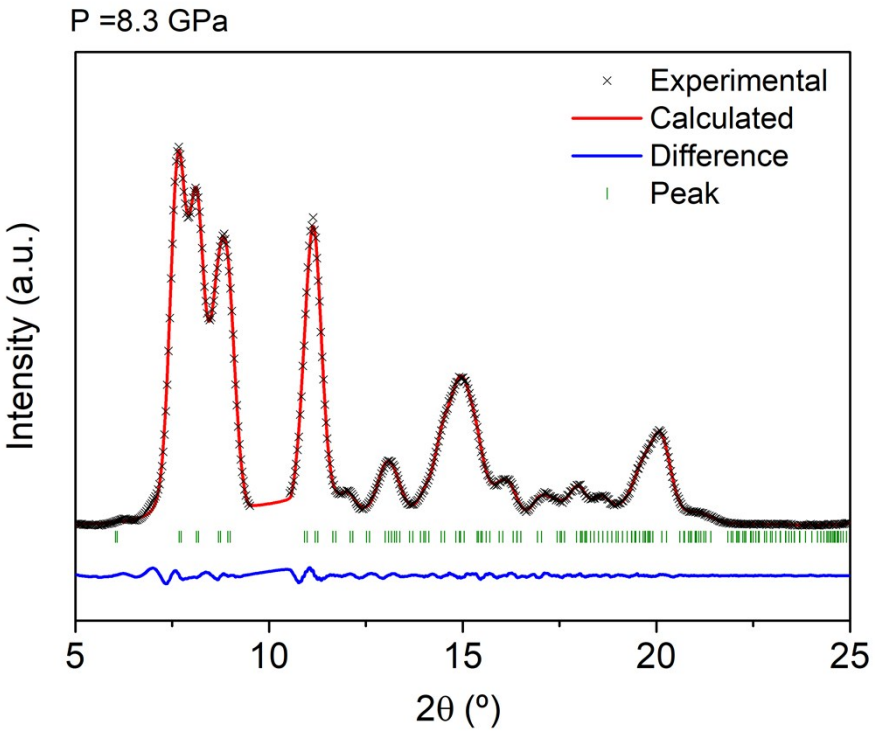

Figure S16. Le Bail fitting of X-ray powder diffraction patterns for the $[NH_4][Cd(HCOO)_3]$ at p = 8.3 GPa to LP-phase. Note: Experimental (black cross), calculated (red solid line) and difference (blue solid line at the bottom) profiles. The tick green marks indicate the positions of the allowed Bragg reflections.

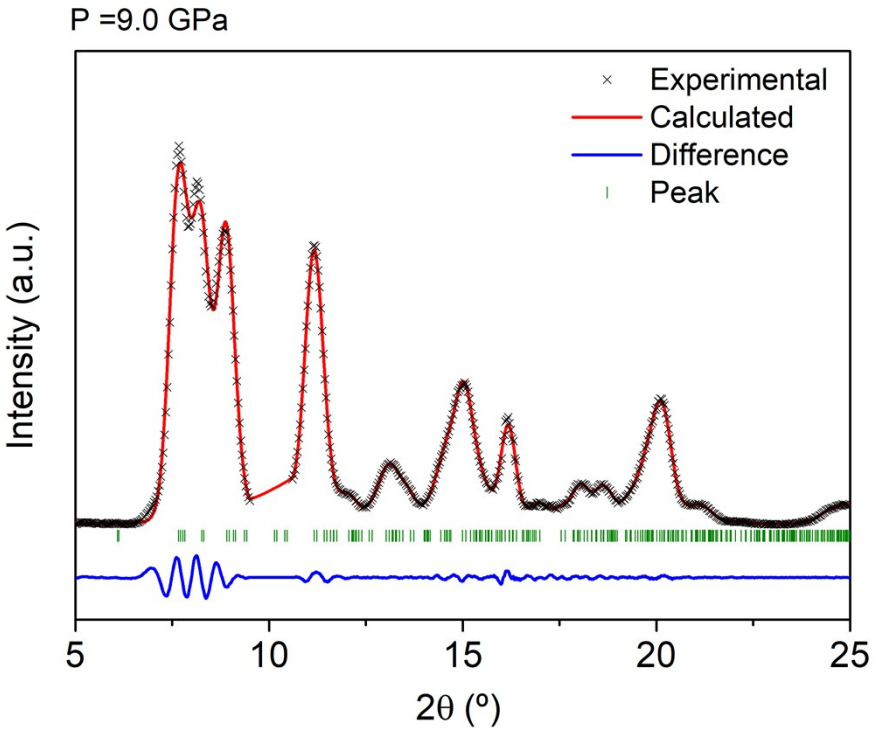

Figure S17. Le Bail fitting of X-ray powder diffraction patterns for the $[NH_4][Cd(HCOO)_3]$ at p = 9.0 GPa to HP-phase. Note: Experimental (black cross), calculated (red solid line) and difference (blue solid line at the bottom) profiles. The tick green marks indicate the positions of the allowed Bragg reflections.

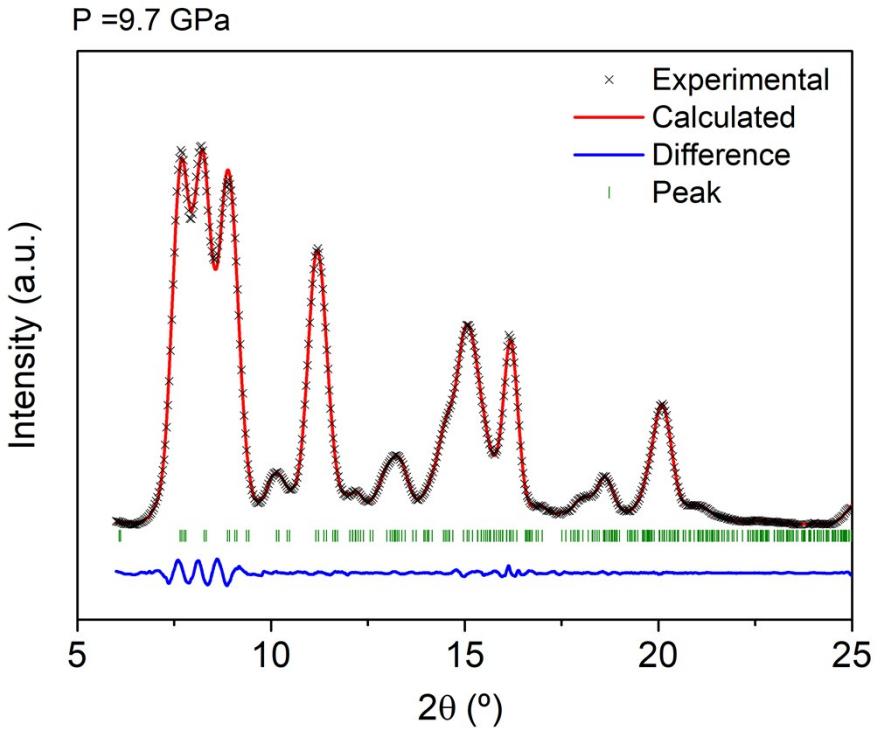

Figure S18. Le Bail fitting of X-ray powder diffraction patterns for the $[NH_4][Cd(HCOO)_3]$ at p = 9.7 GPa to HP-phase. Note: Experimental (black cross), calculated (red solid line) and difference (blue solid line at the bottom) profiles. The tick green marks indicate the positions of the allowed Bragg reflections.

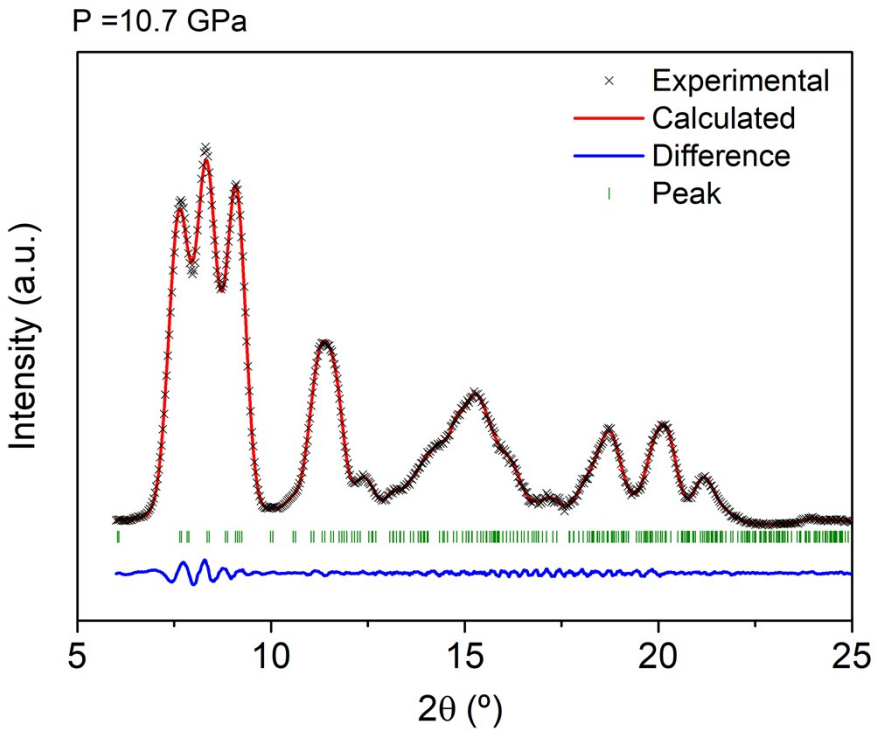

Figure S19. Le Bail fitting of X-ray powder diffraction patterns for the $[NH_4][Cd(HCOO)_3]$ at p = 10.7 GPa to HP-phase. Note: Experimental (black cross), calculated (red solid line) and difference (blue solid line at the bottom) profiles. The tick green marks indicate the positions of the allowed Bragg reflections.

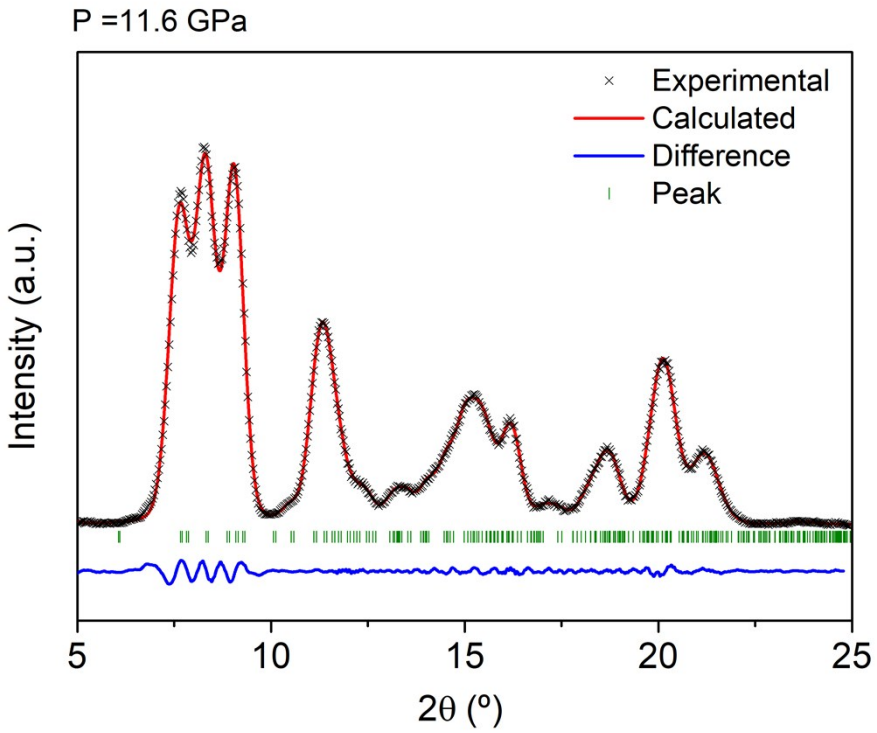

Figure S20. Le Bail fitting of X-ray powder diffraction patterns for the $[NH_4][Cd(HCOO)_3]$ at p = 11.6 GPa to HP-phase. Note: Experimental (black cross), calculated (red solid line) and difference (blue solid line at the bottom) profiles. The tick green marks indicate the positions of the allowed Bragg reflections.

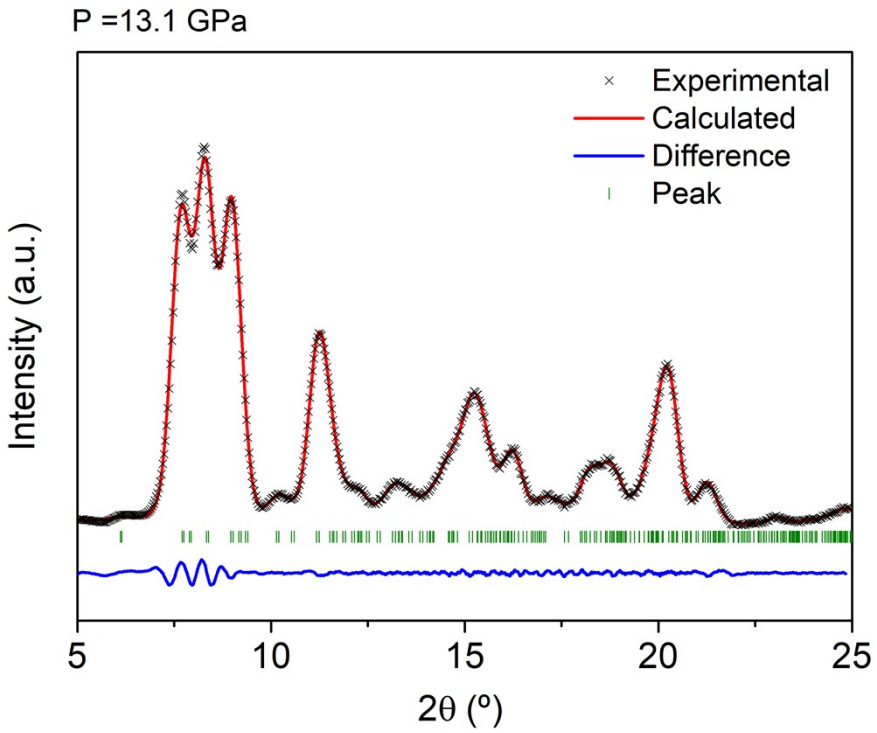

Figure S21. Le Bail fitting of X-ray powder diffraction patterns for the $[NH_4][Cd(HCOO)_3]$ at p = 13.1 GPa to HP-phase. Note: Experimental (black cross), calculated (red solid line) and difference (blue solid line at the bottom) profiles. The tick green marks indicate the positions of the allowed Bragg reflections.

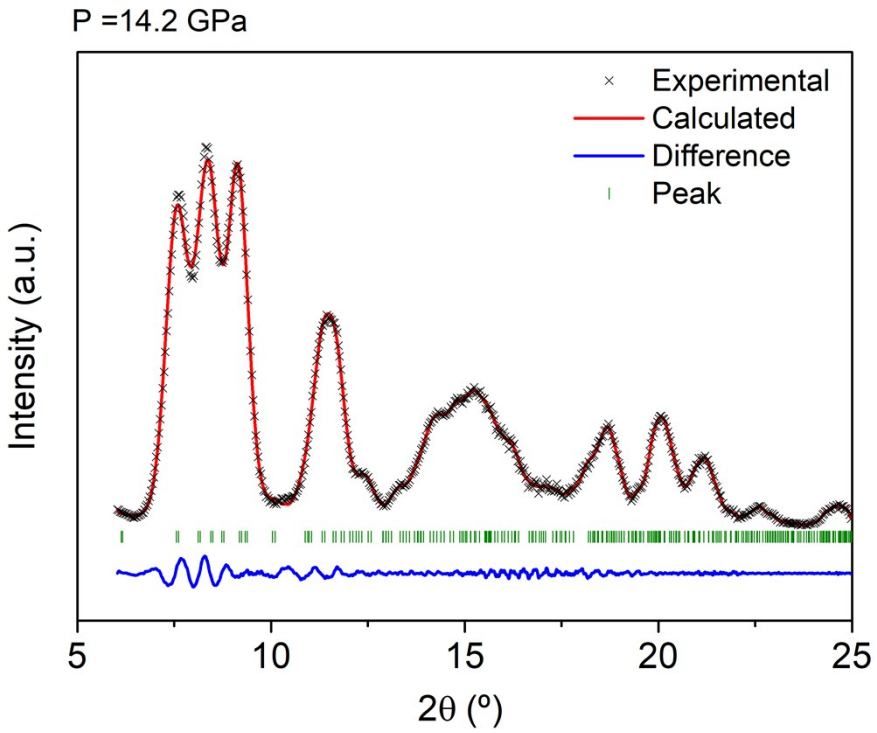

Figure S22. Le Bail fitting of X-ray powder diffraction patterns for the $[NH_4][Cd(HCOO)_3]$ at p = 14.2 GPa to HP-phase. Note: Experimental (black cross), calculated (red solid line) and difference (blue solid line at the bottom) profiles. The tick green marks indicate the positions of the allowed Bragg reflections.

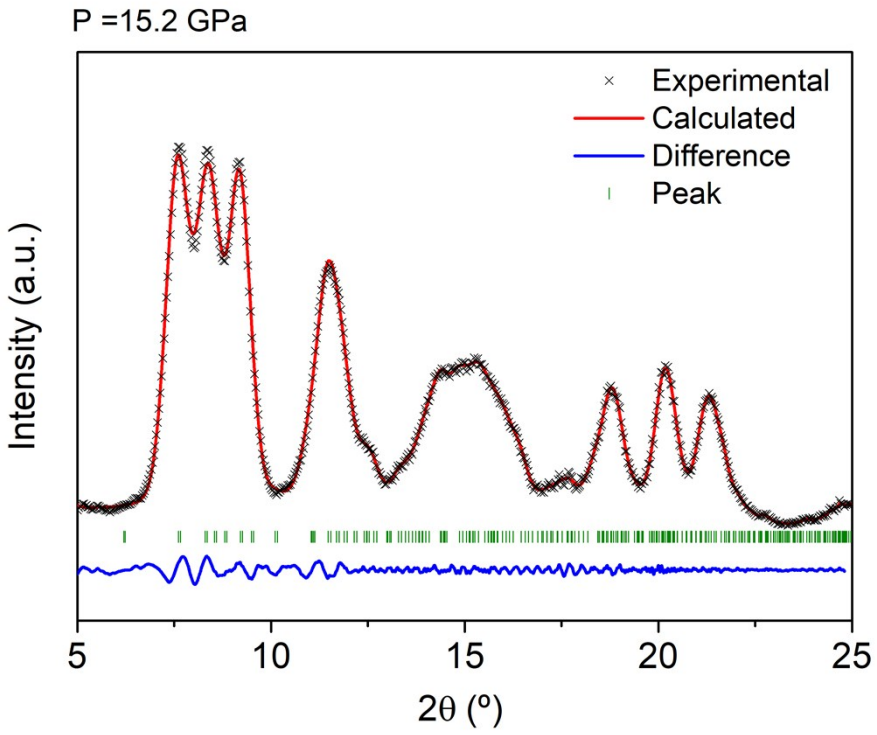

Figure S23. Le Bail fitting of X-ray powder diffraction patterns for the $[NH_4][Cd(HCOO)_3]$ at p = 15.2 GPa to HP-phase. Note: Experimental (black cross), calculated (red solid line) and difference (blue solid line at the bottom) profiles. The tick green marks indicate the positions of the allowed Bragg reflections.

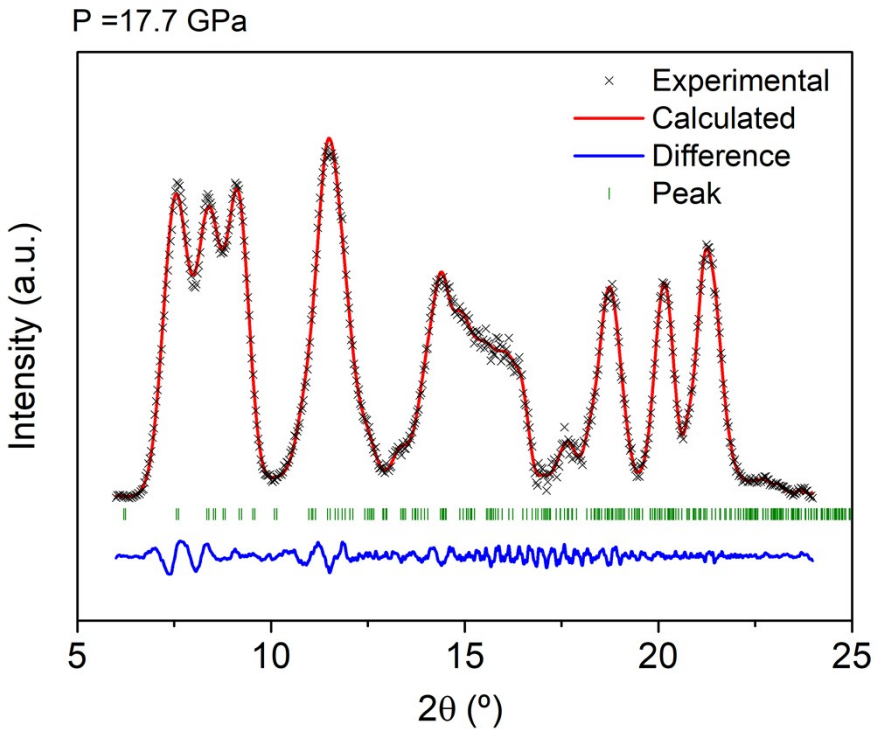

Figure S24. Le Bail fitting of X-ray powder diffraction patterns for the $[NH_4][Cd(HCOO)_3]$ at p = 17.7 GPa to HP-phase. Note: Experimental (black cross), calculated (red solid line) and difference (blue solid line at the bottom) profiles. The tick green marks indicate the positions of the allowed Bragg reflections.

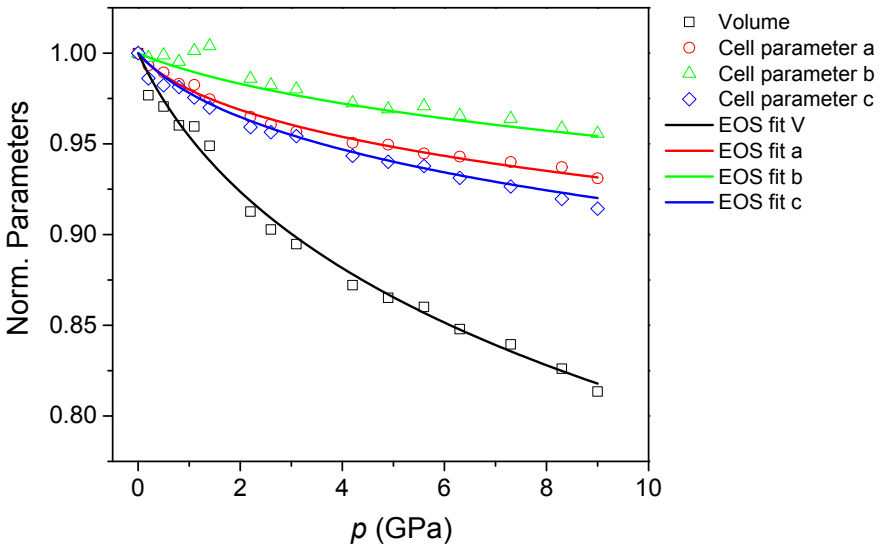

Figure S25. Evolution of the unit cell parameters and volume as a function of pressure for the LP-phase The experimental data obtained from high-pressure PXRD are shown as dots while the solid lines represent the second-order Birch–Murnaghan fits.

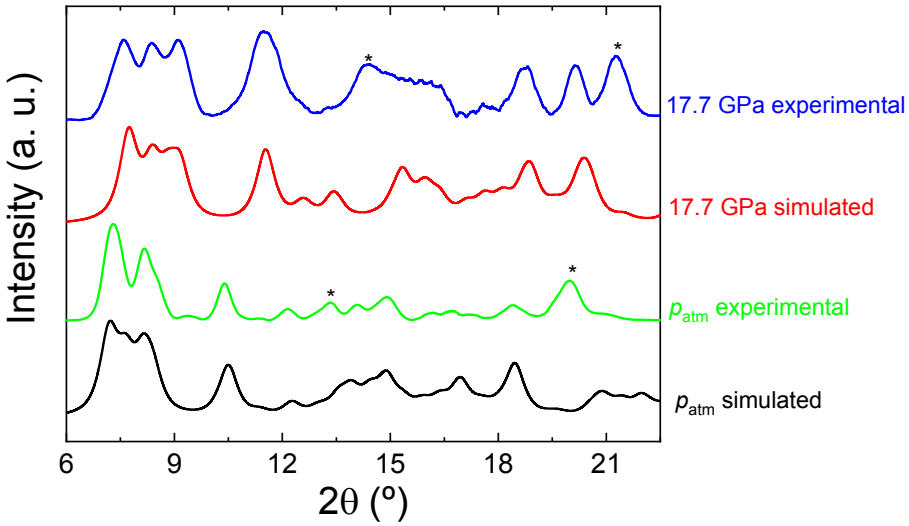

Figure S26. Experimental PXRD patterns for the $[NH_4][Cd(HCOO)_3]$ at atmospheric pressure and 17.7 GPa compared with their simulated profiles from the crystal structures at room temperature. The peaks of the simulated profiles have been anchored to facilitate comparison with the experimental ones. The asterisks show peaks with strong preferred orientation due to the lamellar habit of crystals.

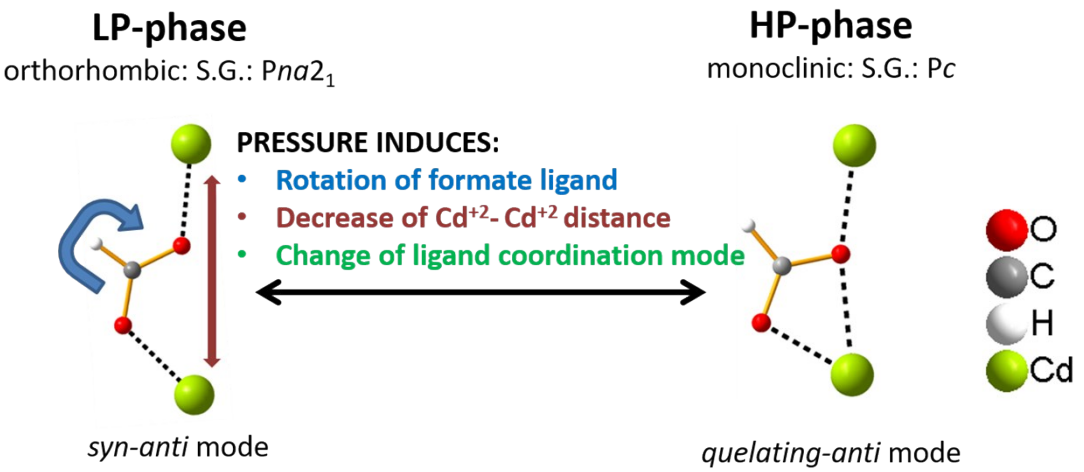

Figure S27. Diagram showing the main changes on the crystal structure caused by external pressure, namely rotation of the formate ligand, change of ligand coordination mode and decrease of the Cd^{2+}-Cd^{2+} distance.

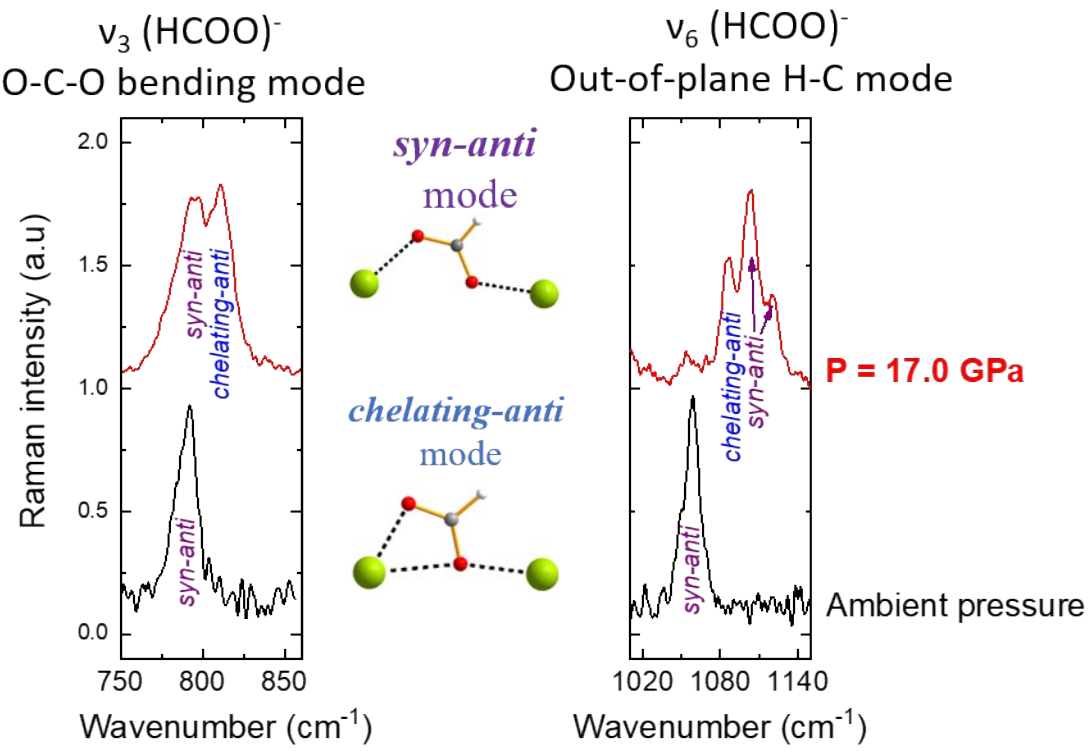

Figure S28. Enlarged view of the experimental Raman spectra at ambient pressure (black line) and P = 17.0 GPa (red line) corresponding to the spectral ranges 750-850 cm^{-1} and 1000-1150 cm^{-1}, where the Raman modes corresponding to the ν_3 ($HCOO_3^-$) (symmetric O-C-O bending) and ν_6 ($HCOO_3^-$) (out of plane H-C mode) can be seen. The vibrational modes have been assigned to the formate ligands in *syn–anti* or *chelating-anti* bridging mode by our DFT calculations**.** For experimental details about the collection of Raman spectra, see reference 31 of manuscript.

Table S1.- Unit cell parameters and R-factors of $[NH_4][Cd(HCOO)_3]$ as a function of pressure as obtained from Le Bail fitting of the PXRD-patterns.

Pressure (GPa)	*a* (Å)	*b* (Å)	*c* (Å)	*Beta* (º)	R_{wp}	R_{exp}
1E-4	6.960(1)	9.507(2)	10.880(2)		5.18%	2.80%
0.2	6.913(1)	9.483(2)	10.728(2)		5.54%	3.09%
0.5	6.886(1)	9.496(1)	10.687(2)		5.17%	3.06%
0.8	6.842(2)	9.462(3)	10.677(3)		11.10%	5.14%
1.1	6.838(1)	9.519(2)	10.614(2)		7.95%	3.91%
1.4	6.783(1)	9.544(2)	10.553(1)		6.52%	4.77%
2.2	6.716(1)	9.374(2)	10.436(1)		6.37%	3.52%
2.6	6.687(2)	9.340(3)	10.406(2)		6.52%	3.72%
3.1	6.659(2)	9.318(2)	10.382(2)		6.42%	4.19%
4.2	6.616(1)	9.245(2)	10.264(1)		5.35%	2.58%
4.9	6.609(2)	9.214(2)	10.228(1)		4.44%	2.31%
5.6	6.575(2)	9.230(2)	10.203(2)		6.47%	3.36%
6.3	6.563(1)	9.180(1)	10.132(1)		7.18%	3.31%
7.3	6.542(1)	9.164(1)	10.080(1)		4.31%	2.49%
8.3	6.523(1)	9.113(1)	10.005(1)		4.34%	2.49%
9	9.862(1)	9.073(2)	6.299(1)	91.47(1)	5.22%	2.67%
9.7	9.826(1)	8.909(1)	6.325(1)	91.27(1)	4.51%	2.22%
10.7	9.769(1)	8.888(1)	6.357(1)	91.34(1)	4.24%	2.60%
11.6	9.770(1)	8.912(1)	6.332(1)	91.02(1)	5.99%	3.39%
13.1	9.787(1)	8.903(1)	6.351(1)	90.97(1)	4.33%	2.43%
14.2	9.747(2)	8.815(1)	6.371(2)	91.80(1)	4.48%	2.90%
15.2	9.719(1)	8.841(1)	6.404(1)	91.45(1)	4.15%	2.64%
17.7	9.690(1)	8.839(1)	6.458(1)	91.78(1)	3.45%	2.70%

Table S2.- Atomic coordinates and lattice parameters of $[NH_4][Cd(HCOO)_3]$ at P=17.7 GPa as obtained from DFT calculations

Space group: P*c*
a=9.3659 Å b=8.5974 Å c= 6.2658 Å β=90.11

C1	0.23716	0.74564	0.23741
C2	0.36746	0.44473	0.04747
C3	0.73638	0.75402	0.76211
C4	0.03631	0.43186	0.14082
C5	0.53693	0.06837	0.85945
C6	0.86836	0.05638	0.95276
Cd1	0.96838	0.74765	0.07576
Cd2	0.46812	0.75322	0.92392
H1	0.80195	0.01889	0.08976
H2	0.19622	0.17997	0.13564
H3	0.60264	0.46958	0.7606
H4	0.10303	0.03122	0.23898
H5	0.33995	0.75315	0.32127
H6	0.8387	0.74499	0.67793
H7	0.30025	0.48248	0.91108
H8	0.69909	0.49812	0.98361
H9	0.19901	0.00291	0.01624
H10	0.78882	0.47252	0.7587
H11	0.2891	0.02727	0.2416
H12	0.13392	0.4893	0.08049
H13	0.63449	0.01037	0.91975
H14	0.69534	0.32076	0.865
N1	0.69642	0.44061	0.84209
N2	0.1968	0.06003	0.15805
O1	0.97381	0.97121	0.90648
O2	0.62252	0.76977	0.65683
O3	0.83338	0.17478	0.85125
O4	0.33241	0.32683	0.14993
O5	0.73632	0.74264	0.96313
O6	0.23639	0.75873	0.03657
O7	0.47379	0.52913	0.09222
O8	0.04722	0.31156	0.2481
O9	0.54813	0.18817	0.75128
O10	0.91846	0.49706	0.09277
O11	0.41887	0.00413	0.90821
O12	0.12366	0.72979	0.34275